Effect of Landauer's blow torch on the equilibration rate in a bistable potential

Mulugeta Bekele,[1] S. Rajesh,[2] G. Ananthakrishna,[2] and N. Kumar[3,4]
[1]*Department of Physics, Addis Ababa University, Addis Ababa, Ethiopia*
[2]*Materials Research Centre, Indian Institute of Science, Bangalore 560 012, India*
[3]*Raman Research Institute, C. V. Raman Avenue, Bangalore 560 080, India*
[4]*Department of Physics, Indian Institute of Science, Bangalore 560 012, India*
(Received 26 June 1998)

The kinetic aspect of Landauer's blow-torch effect is investigated for a model double-well potential with localized heating. Using the supersymmetric approach, we derive an approximate analytical expression for the equilibration rate as a function of the strength, width, and the position of the hot zone, and the barrier height. We find that the presence of the hot zone enhances the equilibration rate, which is found to be an increasing function of the strength and width of the hot zone. Our calculations also reveal an intriguing result, namely, that placing the hot zone away from the top of the potential barrier enhances the rate more than when it is placed close to it. A physically plausible explanation for this is attempted. The above analytical results are borne out by detailed numerical solution of the associated Smoluchowski equation for the inhomogeneous medium. [S1063-651X(99)01301-X]

PACS number(s): 05.40.Jc

I. INTRODUCTION

In a now influential paper [1] on the relative stability, i.e., relative occupation, of the competing local energy minima for a system far from equilibrium, Landauer pointed out the globally determining role played by the nonequilibrium kinetics of the unstable intermediate states even as these are very rarely populated. More specifically, for the case of two local energy minima, i.e., a bistable potential, he showed that the application of localized heating at a point on the reaction coordinate lying between the lower energy minimum and the potential barrier maximum can raise the relative population of the higher-lying energy minimum over that given by the thermal Boltzmann factor $\exp(-\Delta E/k_BT)$. This is the so-called ''blow-torch'' effect [1] associated with a nonuniform thermal bath. It generalizes the problem of escape of a Brownian particle over a potential barrier under the influence of equilibrium thermal fluctuations, studied originally by Kramers [2–4], to the case of nonuniform temperature along the reaction coordinate. Later, in a related context, it has been shown that a state-dependent diffusion coefficient can produce maxima in the probability distribution at points which are not the potential minima [5–7].

A decade later, van Kampen [8] derived an equation appropriate for the description of diffusion in an inhomogeneous medium where he developed a stochastic treatment for the case of nonuniform temperature. Apart from justifying Landauer's conjecture, he also showed that there could be a net current when the particles are allowed to diffuse back through an alternate route bypassing the hot zone. The problem was also treated by Büttiker around the same time [9]. He showed that a net current is possible, even in the absence of an externally applied field, provided both the potential and the state-dependent diffusion constant are periodic with a relative phase difference. Later Landauer [10] considered this aspect of the problem again in light of van Kampen's work. Sinha and Moss [11] have verified Landauer's conjecture by computer simulation. This has also been applied to thermal activation in a superconducting ring with a weak link where transitions produce temperature changes [12]. Indeed, a whole new field of research has emerged centering on the idea of the possibility of directed motion out of noisy states under diverse athermal driving conditions, generically subsumed under ''thermal ratchets'' [13–18], and traceable to the original ''blow-torch theorem'' of Landauer in the sense that the latter may be viewed as injection of noise [19].

Most of the investigations based on the blow-torch effect study the influence of space-dependent temperature on the steady-state relative occupations of the energy minima. To the best of authors' knowledge, there has been no analytical attempt to study the kinetic aspect of the system, specifically, the calculation of the longest relaxation time in a bistable potential in the presence of a blow torch (hot zone). In this work, we address this problem and calculate the equilibration rate for a simple bistable potential with the localized heating positioned somewhere in the (unstable) intermediate region. The associated Smoluchowski equation describing the physical situation will be dealt with using the supersymmetric (SUSY) approach [20–22]. In doing so, we have adapted the supersymmetric potential approach normally applicable to the original Kramers barrier-crossing problem to the case when the temperature is nonuniform along the reaction coordinate.

The rest of the paper is organized as follows. Section II contains a brief introduction to the SUSY method for extracting the longest relaxation rate (i.e., equilibration rate) from the Smoluchowski equation for the case in which temperature is space-dependent. In Sec. III, applying the SUSY method to a model double-well potential with a hot zone, we obtain a matrix equation determining the equilibration rate. In Sec. IV, we present an approximate analytical expression obtained from the matrix equation. The latter is also solved numerically for the sake of comparison. As an independent check for these results, we have solved the Smoluchowski equation numerically and obtained the equilibration rate. The results we obtained from the above three methods for the equilibration rate as a function of different parameters characterizing the hot zone are then discussed. We devote the final section to summary and conclusions.

II. THE METHODOLOGY

The Smoluchowski equation describing the kinetics of a Brownian particle in an inhomogeneous medium is given by [8]

$$\frac{\partial P(x,t)}{\partial t}=\frac{\partial}{\partial x}\left[\mu(x)\left(U'(x)P(x,t)+\frac{\partial}{\partial x}(T(x)P(x,t))\right)\right], \tag{1}$$

where the mobility, μ, and temperature, T, are in general space-dependent. (We take Boltzmann's constant, $k_B=1$.) Here, $P(x,t)$ is the probability density of finding the particle at position x at time t, $U(x)$ describes the potential profile, and the prime on U denotes the derivative with respect to x.

Some remarks on the use of the Smoluchowski equation, Eq. (1), for the case of an inhomogeneous medium are in order at this point as the latter has been a subject of some debate that still continues [8,10,19,23,24]. Landauer has argued [10,19] for a generalization of the Smoluchowski equation where the second term on the right-hand side of Eq. (1) is to be replaced by $P(x,t)(\partial T(x)/\partial x)+\alpha T(x)(\partial P(x,t)/\partial x)$. The parameter α was shown to depend on the physical conditions to be imposed across the temperature discontinuity for no net current. The parameter $\alpha=0.5$ corresponds to a particle interacting with the thermal bath for which the particle velocity is taken to be proportional to $\sqrt{T}$ or $P(x)\propto 1/\sqrt{T(x)}$. On the other hand, $\alpha=1$ corresponds to the case when particles equilibrate via collision (pressure equilibration), i.e., $P(x)\propto 1/T(x)$. However, a direct derivation based on the phase-space Smoluchowski equation by van Kampen gave Eq. (1) corresponding to $\alpha=1$. This is also supported by the work of Jayannavar and Mahato [25] based on a microscopic treatment of the thermal bath as a set of harmonic oscillators. In our work, we will continue to use Eq. (1) for purposes of providing a physically valid description of the problem under consideration.

We consider the case in which temperature is space-dependent but the medium is homogeneous so that the mobility, μ, is taken to be constant. A similar assumption of constant μ has been taken by Sinha and Moss in their work [11]. Then, the corresponding Smoluchowski equation is

$$\frac{\partial P(x,t)}{\partial t}=\mu\frac{\partial}{\partial x}\left[U'(x)P(x,t)+\frac{\partial}{\partial x}(T(x)P(x,t))\right]. \tag{2}$$

The stationary solution of Eq. (2) is given by

$$P_{\mathrm{ss}}(x)=\frac{C}{T(x)}\exp\left[-\int_{-\infty}^{x}\frac{U'(\tilde{x})}{T(\tilde{x})}d\tilde{x}\right], \tag{3}$$

where C is the normalization constant. In this work, we choose a simple temperature profile whose value is *constant* both outside and inside the hot zone with $T=T_0$ and $T=T_0+T_b$, respectively, where T_b is the excess temperature above the constant background value T_0. [See Eq. (10).] Using the transformation

$$P(x,t)=\frac{\phi(x)}{T(x)}\exp\left[-\int_{-\infty}^{x}\frac{U'(\tilde{x})}{2T(\tilde{x})}d\tilde{x}\right]e^{-\lambda t}, \tag{4}$$

we convert Eq. (2) to a Euclidean Schrödinger equation

$$H_+\phi_+=A^+A\phi_+=E_+\phi_+ . \tag{5}$$

Here, $E_+=\lambda/\mu T_0$ and the operators A and A^+ are given by

$$A=\frac{f\partial}{\partial x}+\frac{U'(x)}{2fT_0}, \quad A^+=-\frac{f\partial}{\partial x}+\frac{U'(x)}{2fT_0}. \tag{6}$$

In Eq. (6), the parameter f reflects the excess temperature defined by $f=\sqrt{1+s}$, with $s=T_b/T_0$. Thus, for the interval of x outside the hot zone, the corresponding operators have $f=1$. The Hamiltonian H_+ corresponds to the motion of a particle in the potential

$$V_+(x)=\left(\frac{U'(x)}{2T(x)}\right)^2-\frac{U''(x)}{2T(x)}. \tag{7}$$

For a high barrier, the longest relaxation rate is determined by the smallest nonzero eigenvalue λ_1 associated with the first excited state of Eq. (5). On the other hand, this eigenstate is degenerate with the ground state ϕ_-^0 of the ''supersymmetric partner potential'' $V_-(x)$ given by

$$V_-(x)=\left(\frac{U'(x)}{2T(x)}\right)^2+\frac{U''(x)}{2T(x)}, \tag{8}$$

such that

$$H_-\phi_-^0=AA^+\phi_-^0=E_-\phi_-^0, \tag{9}$$

where $E_-=\lambda_1/\mu T_0$. Thus, the problem of finding the equilibration rate amounts to finding the ground-state eigenvalue of this ''partner'' potential. It is worth pointing out here that for the temperature profile we use, we *exclude* the two points where $T(x)$ is discontinuous. However, following the line of attack used for obtaining the solution of the Schrödinger equation in the presence of a δ-function potential, we devise a technique of relating the wave functions on either side of these points (see the Appendix).

Here we would like to mention that the SUSY method is a powerful analytical method used for simple model potentials such as the W potentials. The applicability for calculating Kramers' escape rate in a W potential for a *uniform* temperature case has been demonstrated by Schönhammer [22]. We found this method to be particularly useful while investigating the influence of barrier subdivision on the escape rate, where we have demonstrated the existence of the optimal number of subdivisions that maximizes the escape rate [26].

III. THE MODEL AND ITS SOLUTION

We consider a simple bistable potential in the form of a symmetric W potential which is piecewise linear having the same magnitude in slope. It is described by the barrier height U_0 and the distance $2L_0$ between the two potential minima located at $x=\pm L_0$ on either side of the origin [Fig. 1(a)]. The localized hot zone of a certain width is taken to be

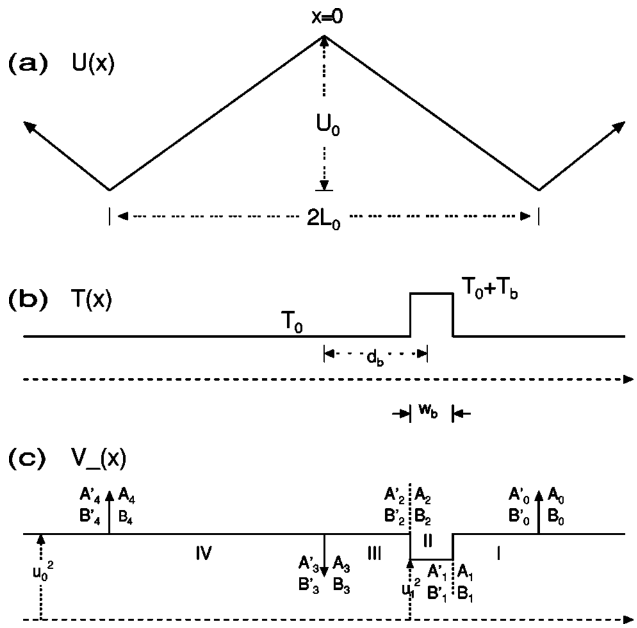

FIG. 1. (a) The W potential, (b) temperature profile $T(x)$, having the hot zone, (c) SUSY partner potential, $V_-(x)$.

positioned somewhere between the two potential minima. We assume a simple temperature profile of the following form for the heat bath:

$$T(x)=T_0+T_b\left[\Theta\left(x-d_b+\frac{w_b}{2}\right)-\Theta\left(x-d_b-\frac{w_b}{2}\right)\right]. \tag{10}$$

Here, $\Theta(x)$ is the Heaviside function, T_0 is the background (constant) temperature, and T_b is the excess temperature of the hot zone. The parameters d_b and w_b specify, respectively, the distance of the midpoint of the hot zone from the barrier top and the width of the hot zone [Fig. 1(b)].

The corresponding supersymmetric ''partner'' potential $V_-(x)$ with the hot zone is given by

$$V_-(x)=\frac{2u_0}{L_0}[\delta(x+L_0)-\delta(x)+\delta(x-L_0)]+\left(\frac{u_{0,1}}{L_0}\right)^2. \tag{11}$$

This relation holds well at all points *except* at the two points of temperature discontinuity. Here, $u_0=U_0/2T_0$ and $u_1=u_0/(1+s)$. It is clear that the potential $V_-(x)$ takes a constant value $(u_0/L_0)^2$ *outside* the hot zone and $(u_1/L_0)^2$ *within*. Three additional δ-function potentials (two repulsive and one attractive) are superposed at different locations as shown in Fig. 1(c). Changing the variable x to $y=x/L_0$ gives a new dimensionless Hamiltonian $h_-=L_0^2H_-$ such that

$$h_-\phi_-^0(y)=e_b\phi_-^0(y), \tag{12}$$

whose potential is

$$V_-(y)=2u_0[\delta(y+1)-\delta(y)+\delta(y-1)]+(u_{0,1})^2. \tag{13}$$

Here, e_b is a dimensionless quantity equal to $L_0^2E_-$ or equivalently $L_0^2\lambda_1/\mu T_0$. In the scaled form, the position of the midpoint of the hot zone from the top of the barrier and the width of the hot zone are defined by $d=d_b/L_0$ and $w=w_b/L_0$, respectively. Henceforth, we use only the scaled variables. The transfer-matrix method has been used to find the equation governing the eigenvalue e_b. Below, we outline the procedure leaving the details to the Appendix.

The ground-state wave function, ϕ_-^0, is taken to have the form $A_ne^{-k(y-y_n)}+B_ne^{k(y-y_n)}$ located with respect to the positions $y=y_n$ of each of the δ-function potentials and at points of discontinuity in the temperature profile. The amplitudes A_n, B_n and A'_n, B'_n on either side of these special points are shown in Fig. 1(c). For regions outside the hot zone, the wave vector k is given by

$$k_0=\sqrt{u_0^2-e_b}, \tag{14}$$

while for within the hot zone it is given by

$$k_1=\sqrt{u_1^2-\frac{e_b}{1+s}}. \tag{15}$$

The amplitudes A'_4 and B'_4 that appear just on the left side of the positive δ-function potential located at $y=-1$ are related to A_0 and B_0, which appear on the right side of the positive δ-function potential located at $y=1$ through a transfer matrix **M**, such that

$$\begin{pmatrix}A'_4\\ B'_4\end{pmatrix}=\mathbf{M}\begin{pmatrix}A_0\\ B_0\end{pmatrix}. \tag{16}$$

The matrix **M** is the product of successive transfer matrices which are derived in the Appendix. Since we are looking for a bound state solution, $A'_4=B_0=0$. This implies that the 11-matrix element of **M** must be zero, i.e.,

$$M_{11}=0, \tag{17}$$

the solution of which gives the value of e_b and, hence, the equilibration rate.

IV. RESULTS AND DISCUSSION

The effect of the hot zone on the equilibration rate for the given potential is studied in terms of the three parameters characterizing the hot zone: (i) the relative degree of hotness of the hot zone with respect to the rest of the heat bath, $s=T_b/T_0$, (ii) the scaled width of the hot zone, $w=w_b/L_0$, and (iii) the scaled distance of the hot zone from the top of the potential barrier, $d=d_b/L_0$. Since the hot zone is in between the top of the barrier and the right minimum, the parameters d and w can only take values between 0 and 1. On the other hand, the strength s can take positive values for the hot zone and negative values (greater than -1) for the *cold* zone. In addition, for each of these cases we have studied the influence of the barrier height $u_0=U_0/2T_0$ on the equilibration rate.

The change in the equilibration rate due to the presence of the hot zone is better appreciated in terms of a quantity which we call the *enhancement factor*, f_b, and defined by

$$f_b = \frac{e_b}{e_0}, \tag{18}$$

where e_0 stands for e_b when there is no hot zone $(s=0)$. f_b physically represents the factor by which the equilibration rate improves due to the presence of the hot zone.

An expression for the enhancement factor in terms of all the relevant parameters can be found from Eq. (17). By noting that, for a high barrier, k_0 and k_1 can be expanded about u_0 and u_1, respectively, we find the enhancement factor to be approximately given by

$$f_b = \frac{\exp(s\sigma)\cosh(s\sigma)}{1+s\exp(s\sigma)\sinh(\sigma)\exp(-2u_0 d)}, \tag{19}$$

where $\sigma \equiv w u_0/(1+s)$. Even though this equation gives very accurate values comparable to those obtained by numerically solving Eq. (17), the above equation can be further approximated into a more transparent form when the hot zone is located halfway down the top $(d=0.5)$ and is given by

$$f_b = \frac{1}{2}\left[1+\exp\left(2u_0 w \frac{s}{1+s}\right)\right]. \tag{20}$$

Equation (20) shows that for a given barrier height u_0 and width w, f_b increases as the strength of the hot zone, s, increases and saturates for large values. In addition, the enhancement factor f_b has an exponential dependence on both the width w of the hot zone and the barrier height u_0. It may be noted that the above expression has the correct limiting behavior as a function of both $s \to 0$ and $w \to 0$. Equation (19) shows that the enhancement factor f_b saturates as the blow torch is moved away from the top of the potential barrier.

As an independent check of the analytical results [Eq. (19)], we have numerically solved Eq. (2) for a given temperature and potential parameters. Before numerically obtaining f_b, we have studied the evolution of the probability distribution towards the steady state. This was done by using an initial probability distribution sharply peaked around the bottom of the right well. A three-dimensional plot of the time evolution of the probability distribution towards the steady state is shown in Fig. 2(a). The numerically obtained asymptotic steady-state distribution is shown in Fig. 2(b). This clearly has a higher population in the left well than the right, which in the absence of the hot zone would be symmetric about the origin. Our numerical results show that this asymptotic distribution is practically identical with the steady-state distribution $P_{ss}(y)$ in terms of the scaled variable.

One direct method of determining *the long time decay rate* of the probability distribution is to allow the system to evolve for long enough time towards the steady state. At late stages when the probability distribution is observed not to show any appreciable change, we can calculate the decay rate by plotting the *total* probability on the right well as a function of time (on $\ln t$ scale). However, it must be mentioned here that for calculating the equilibration rate, a more efficient way is to take the initial distribution to be a distribution which is *marginally* different from the stationary distribution [given by Eq. (3)]. Even so, high values of u_0 (~ 10) take long computer time for the system to reach the near station-

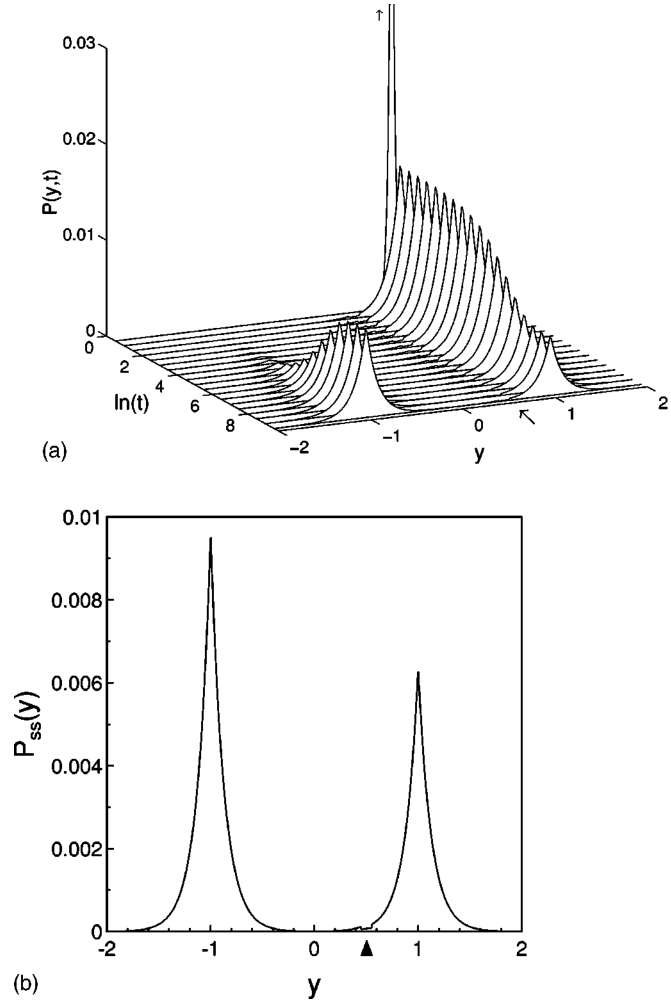

FIG. 2. (a) Time evolution of the probability distribution $P(y,t)$, towards the steady state for a given temperature. The parameter values are $s=1.0$, $u_0=4$, $w=0.1$, and $d=0.5$. (b) Very late stage probability distribution obtained by numerically integrating Eq. (2) taken as the steady-state distribution. Note the dip in the probability value at the location of the hot zone shown by an arrow.

ary state required for calculating the equilibration rate. For this reason, for the numerical works based on Eq. (2) we have limited our calculation to $u_0=4$. Although this value of u_0 satisfies the high barrier condition, it is on the low side.

We now consider the influence of the hot zone on the equilibration rate. We shall refer to the results obtained from the approximate analytic expression [Eq. (19)] as analytical results, exact results obtained by numerically solving the root of the equation [Eq. (17)] as semianalytical results, and the results obtained by numerically solving Eq. (2) as numerical results. Figure 3 shows plots of the enhancement factor f_b versus strength of the blow torch s for various values of the barrier height u_0 placing the blow torch (of width $w=0.1$) midway from the top of the potential $(d=0.5)$. (The set of curves a, b, and c refer to three different values of the barrier height $u_0=4$, 10, and 15, respectively.) We have shown the analytical results by a dashed line, the semianalytical results by a continuous line, and the numerical results by filled circles. (For higher values of u_0, we have shown only the analytical results and semianalytical results, since numerical results are time consuming.) As can be seen from Fig. 3, for

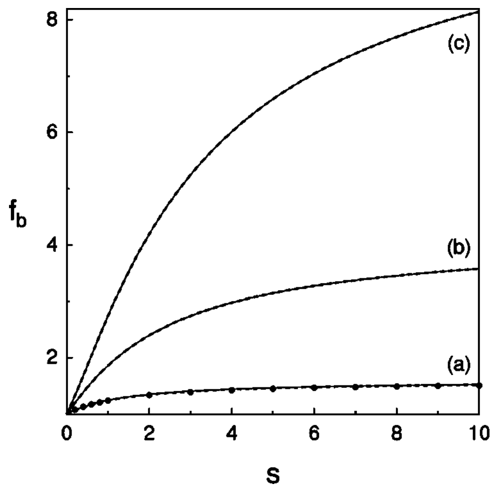

FIG. 3. Plot of f_b versus s, for $d=0.5$, and $w=0.1$ for the values of (a) $u_0=4$, (b) $u_0=10$, and (c) $u_0=15$. Dashed lines correspond to the results from Eq. (19), solid lines to the semianalytical method, and filled circles to numerical solution.

higher values of the barrier height u_0, analytical results are not distinguishable from the semianalytical results over the entire range of s. This clearly reflects the fact that large u_0 approximation made in obtaining Eq. (19) holds well. Consider the dependence of f_b on the width of the hot zone w. Figure 4 shows plots of f_b as a function of w for $u_0=4$, 10, and 15 labeled by (a), (b), and (c), respectively, for $s=1$ and keeping the blow torch halfway down the barrier top, i.e., $d=0.5$. As before, for $u_0=4$, where we have numerical results there is excellent agreement between the numerical results, and analytical and semianalytical results over the entire range of w. For $u_0=10$ and 15, semianalytical results are indistinguishable from the analytical results. Lastly, we consider the dependence of the enhancement factor, f_b, on the position of the hot zone from the barrier top, d. Figure 5 shows plots of f_b versus d for $u_0=4$, 10, and 15 denoted by (a),(b), and (c), respectively (keeping the strength of the hot zone $s=1$ and its width $w=0.1$). For relatively low barrier

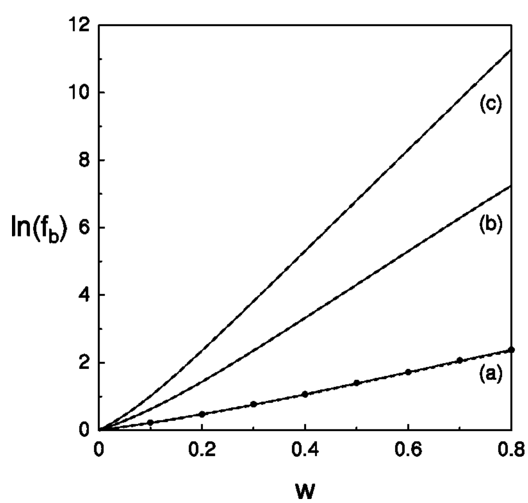

FIG. 4. Three plots of f_b versus w, for $d=0.5$, and $s=1$ for the values of (a) $u_0=4$, (b) $u_0=10$, and (c) $u_0=15$. Dashed lines correspond to the results from Eq. (19), solid lines to the semianalytical method, and filled circles to numerical solution.

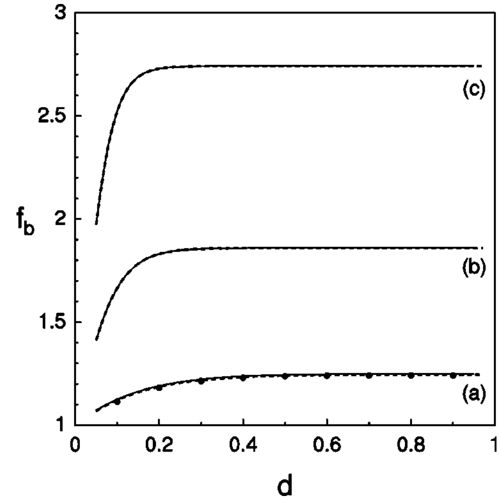

FIG. 5. Plots of f_b versus d for $s=1.0$, and $w=0.1$ for the values of (a) $u_0=4$, (b) $u_0=10$, and (c) $u_0=15$. Dashed lines correspond to the results from Eq. (19), solid lines correspond to semianalytical results, and filled circles to numerical solution.

height, $u_0=4$, we see that the analytical results agree well with the semianalytical results and the numerical results. Unlike for small barrier height, for which f_b saturates slowly, for large barrier heights [(b) and (c)], f_b saturates quickly and stays nearly constant beyond $d\sim0.2$. Here again, the analytical results agree very well with the semianalytical results. The above results reveal that the equilibration rate is higher when the hot zone is *away* from the barrier top.

The above dependence of enhancement factor (f_b) for the equilibration rate on the position of the blow torch (d), shown in Fig. 5, is intriguing. The enhancement factor is seen to saturate quickly (to a value greater than unity) as the blow torch moves away from the barrier top (i.e., as d increases beyond T_0/U_0), while it decreases towards unity as the blow torch approaches the top of the potential barrier. (Of course, for sufficiently small d, the hot zone begins to bracket the potential maximum because of finite width.) The above general feature may be physically understood in terms of an argument due to Landauer [27] based on the equilibration rate, $1/\tau=1/\tau_L+1/\tau_R$, for the occupation of the two wells, where τ_L and τ_R refer to the time for crossing the barrier from the left and from the right, respectively. Thus, for a blow torch on the right side of the barrier, we expect not only τ_R to increase as we approach the top of the barrier (as d decreases), but also τ_L should increase as the particles crossing the barrier from the left well will be returned back by the blow torch. This might qualitatively explain the result of d dependence of the enhancement factor, f_b. However, this argument does not enable us to estimate the relative importance of the two effects, namely, the variation of τ_L and τ_R with d. To clarify this point, we have carried out calculation of τ for a highly asymmetric double-well potential in the limit of a very deep right well. We considered two cases: (i) when the hot zone is placed to the right of the barrier top and (ii) when it is to the left. This enabled us to isolate to a very good approximation the d dependence of τ_L and τ_R, respectively, from $\tau(d)$. *Our finding is that the decrease in the enhancement factor, f_b, as d decreases is* *dominated by the increase of τ_R, although τ_L also increases weakly*. This is somewhat counterintuitive.

V. SUMMARY AND CONCLUSIONS

In summary, we have been able to study the kinetic aspect of Landauer's blow-torch theorem using the supersymmetric approach and using a simple model W potential. The choice of the W potential is particularly well adapted to the SUSY method. Our analysis shows that the rate of equilibration is substantially improved due to the presence of the hot region. The exact magnitude depends on its strength, its width, its location, and also on the barrier height. We have also obtained an approximate analytical expression for the equilibration rate from transfer matrices derived using the SUSY method. These results agree well with the results obtained by numerical solution of the associated Smoluchowski equation.

We expect that the present analysis would be useful in understanding some problems when local heating is viewed in a more general context of local noise injection. Viewed from this angle, these results are clearly applicable even when fluctuations are athermal. One example where athermal fluctuations play an important role is the depinning of dislocation segments from obstacles resulting in movement of dislocations [28]. Another example where the present analysis may be useful is the study of kinetics of phase transformations. In this case, the free energy takes the role of the potential and the order parameter takes the role of the reaction coordinate. However, it is worth pointing out that, in general, subjecting a range of order parameter values to excess heating is not easy since there is no correspondence between the values taken by the order parameter and its location in space. In this context, martensite transformation offers a promising physical situation in which we are actually dealing with the free energy in terms of strain order parameter. It would be interesting to realize the applicability of the present analysis to some experimental situations.

ACKNOWLEDGMENTS

The authors would like to thank Professor Rolf Landauer for very insightful comments. One of the authors (M.B.) would like to thank The International Program in Physical Sciences, Uppsala University, Uppsala, Sweden for financial support for this work. He would also like to thank the Indian Institute of Science, particularly the Materials Research Center Theory Group, for providing the necessary research facilities.

APPENDIX

In this appendix we outline the method of evaluating the matrix $\mathbf{M}$ that relates the amplitudes A_4', B_4' of ϕ_-^0 found on the left side of the δ-function potential at $y=-1$ to the amplitudes A_0, B_0 found on the right side of the δ-function potential at $y=1$. [See Fig. 1(c).]

The region of the W potential has four intervals of constant potential $V_-(x)$ marked by I, II, III, and IV as shown in Fig. 1(c). In these intervals, only simple phase changes in the wave function occur. In contrast, the wave function changes in a significant way across regions of temperature discontinuity and at points where δ functions are present. First, consider the phase changes which are simple to evaluate. The pairs of amplitudes A_{n+1} and B_{n+1} at the left end of these regions (I to IV) are related to those at the right end, A_n' and B_n', through the matrix equation

$$\begin{pmatrix} A_{n+1} \\ B_{n+1} \end{pmatrix} = \mathbf{P}(a) \begin{pmatrix} A_n' \\ B_n' \end{pmatrix}, \tag{A1}$$

where

$$\mathbf{P}(a) = \begin{pmatrix} e^{-ka} & 0 \\ 0 & e^{ka} \end{pmatrix}. \tag{A2}$$

Here a stands for the width of the concerned interval and k is either k_0 or k_1 depending on whether the interval is outside or within the hot zone.

Now, consider relating the amplitudes across the points of discontinuity in the temperature profile. The probability density $P(y,t)$ which is related to $\phi_-^0(y)$ through the transformation Eq. (4), is a continuous function of the position *including* the two points where temperature is discontinuous. Therefore, $\phi_-^0(y)$ on either side of these two points must be discontinuous in such a way that $P(y,t)$ remains continuous. In particular, at $y_1 = d + w/2$, using Eq. (3) and using the continuity condition $P(y_1^+,t) = P(y_1^-,t)$, we get

$$\phi_-^0(y_1^+) = \frac{\phi_-^0(y_1^-)}{(1+s)}. \tag{A3}$$

Here $y_1^\pm = y_1 \pm \epsilon$ with $\epsilon \to 0$.

The second relation between the amplitudes comes from integrating the SE equation across y_1 and exploiting the continuity of $P(y,t)$. This leads to the continuity of $\partial(TP)/\partial y$. At $y=y_1$, this implies that

$$(\phi_-^0(y_1^+))' = (\phi_-^0(y_1^-))', \tag{A4}$$

where the primes denote the spatial derivative. Using Eqs. (A3) and (A4), the pairs of amplitudes A_1, B_1 and A_1', B_1' found on the two sides of the discontinuous temperature profile located at y_1 are related through the equation

$$\begin{pmatrix} A_1' \\ B_1' \end{pmatrix} = \mathbf{M}_1 \begin{pmatrix} A_1 \\ B_1 \end{pmatrix}, \tag{A5}$$

where

$$\mathbf{M}_1 = \frac{1}{2k_1} \begin{pmatrix} (1+s)k_1 + k_0 & (1+s)k_1 - k_0 \\ (1+s)k_1 - k_0 & (1+s)k_1 + k_0 \end{pmatrix}. \tag{A6}$$

In the same way, the two sets of amplitudes A_2, B_2 and A_2', B_2' found on the two sides of the discontinuous temperature profile located at $y_2 = d - w/2$ are related through the matrix equation

$$\begin{pmatrix} A_2' \\ B_2' \end{pmatrix} = \mathbf{M}_2 \begin{pmatrix} A_2 \\ B_2 \end{pmatrix}, \tag{A7}$$

where

$$\mathbf{M}_2 = \frac{1}{2(1+s)k_0}\begin{pmatrix} k_0+(1+s)k_1 & k_0-(1+s)k_1 \\ k_0-(1+s)k_1 & k_0+(1+s)k_1 \end{pmatrix}. \tag{A8}$$

We are now left with relating the amplitudes on either sides of the three δ-function potentials located at $y=-1$, 0, and 1. At all these three δ functions, ϕ_-^0 is continuous since temperature is continuous. Thus, the pairs of amplitudes A_0, B_0 and A_0', B_0' on the right and the left sides of the δ function located at $y=1$ are related through

$$A_0' + B_0' = A_0 + B_0. \tag{A9}$$

Integrating the Euclidean Schrödinger equation across this positive δ function with the width of the integration tending to zero give a second relation between these amplitudes:

$$A_0' - B_0' = -\frac{2u_0}{k_0}(A_0+B_0) + A_0 - B_0. \tag{A10}$$

These two relations give a matrix equation relating the two sets of amplitudes:

$$\begin{pmatrix} A_0' \\ B_0' \end{pmatrix} = \mathbf{M}_+ \begin{pmatrix} A_0 \\ B_0 \end{pmatrix}. \tag{A11}$$

The same transfer matrix $\mathbf{M}_+$ also relates the pairs of amplitudes A_4', B_4' to A_4, B_4 since features around $y=1$ are identical to those around $y=-1$. When relating the pairs of amplitudes A_3, B_3 to A_3', B_3' corresponding to the two sides of the δ function located at $y=0$, we note that the only difference is that the sign of the δ function is negative. Going through the same procedure as above, we get the matrix equation

$$\begin{pmatrix} A_3' \\ B_3' \end{pmatrix} = \mathbf{M}_- \begin{pmatrix} A_3 \\ B_3 \end{pmatrix}. \tag{A12}$$

The transfer matrices $\mathbf{M}_\pm$ are given by

$$\mathbf{M}_\pm = \frac{1}{k_0}\begin{pmatrix} k_0 \mp u_0 & \mp u_0 \\ \pm u_0 & k_0 \pm u_0 \end{pmatrix}. \tag{A13}$$

Using all the transfer matrices relating the successive sets of amplitudes, the matrix $\mathbf{M}$ is given by

$$\mathbf{M} = \mathbf{M}_+ \mathbf{P}(1) \mathbf{M}_- \mathbf{P}\left(d - \frac{w}{2}\right) \mathbf{M}_2 \mathbf{P}(w) \mathbf{M}_1 \mathbf{P}\left(1 - d - \frac{w}{2}\right) \mathbf{M}_+ . \tag{A14}$$

[1] R. Landauer, Phys. Rev. A **12**, 636 (1975).
[2] H. A. Kramers, Physica (Amsterdam) **7**, 284 (1940).
[3] P. Hanggi, P. Talkner, and M. Borkovec, Rev. Mod. Phys. **62**, 251 (1990).
[4] V. I. Mel'nikov, Phys. Rep. **209**, 1 (1990).
[5] W. Horthemke and R. Lefever, Phys. Lett. **64A**, 19 (1977).
[6] R. Landauer, Phys. Lett. **68A**, 15 (1978).
[7] D. Ryter, Z. Phys. B **41**, 39 (1981).
[8] N. G. van Kampen, IBM J. Res. Dev. **32**, 107 (1988).
[9] M. Büttiker, Z. Phys. B **68**, 161 (1987).
[10] R. Landauer, J. Stat. Phys. **53**, 233 (1988).
[11] K. Sinha and F. Moss, J. Stat. Phys. **54**, 1411 (1989).
[12] D. W. Bol and R. De Bruyn Ouboter, Physica B **154**, 56 (1988); **160**, 56 (1989).
[13] K. Svoboda, C. F. Schmitt, B. J. Schnapp, and S. M. Block, Nature (London) **365**, 721 (1993).
[14] R. B. Bartussek, P. Hänggi, and J. G. Kissner, Europhys. Lett. **28**, 459 (1994).
[15] R. D. Astumian and M. Bier, Phys. Rev. Lett. **72**, 1766 (1994).
[16] C. B. Doering, W. Horthemke, and J. Riordan, Phys. Rev. Lett. **72**, 2984 (1994).
[17] M. C. Mahato and A. M. Jayannavar, Phys. Lett. A **209**, 21 (1995).
[18] D. R. Chialvo and M. M. Millonas, Phys. Lett. A **209**, 26 (1995).
[19] R. Landauer, in *Fluctuations and Order: The New Synthesis*, edited by M. Millonas (Springer, Heidelberg, 1996) .
[20] M. Bernstein and L. S. Brown, Phys. Rev. Lett. **52**, 1933 (1984).
[21] H. R. Jauslin, *Lecture Notes in Physics* (Springer-Verlag, Berlin, 1988), Vol. 319, p. 97.
[22] K Schönhammer, Z. Phys. B **78**, 63 (1990).
[23] R. Landauer, Helv. Phys. Acta **56**, 847 (1983).
[24] N. G. van Kampen, Z. Phys. B **68**, 135 (1987).
[25] A. M. Jayannavar and Mangal Mahato, Pramana, J. Phys. **45**, 369 (1995).
[26] Mulugeta Bekele, G. Ananthakrishna, and N. Kumar, Pramana, J. Phys. **46**, 403 (1996).
[27] R. Landauer (private communication).
[28] Mulugeta Bekele, Ph.D. thesis, Indian Institute of Science, Bangalore, 1997 (unpublished).